Cross Correlations between the Radiation and Atmospheric Variables in a General Circulation Model and in Satellite Data

THOMAS P. CHARLOCK

Atmospheric Sciences Division, NASA Langley Research Center, Hampton, Virginia

FRED G. ROSE AND KAREN M. CATTANY-CARNES

Aero-Space Technologies Division, PRC Kentron, Hampton, Virginia

(Manuscript received 1 April 1988, in final form 1 August 1988)

ABSTRACT

The classical picture of the influence of midlatitude troughs on cloud patterns is investigated in a general circulation model (GCM) and in satellite and National Meteorological Center (NMC) data by comparing the cross correlation of the poleward component of the wind and the outgoing longwave radiation (OLR). The GCM simulation is found to compare quite well with data for the bandpass (2.5- to 6-day) waves over the midlatitudes. Over the storm tracks, a significant portion of the variance of the OLR is explained by a correlation with the poleward component of the horizontal wind; this is forced, as expected, by stronger correlations with the vertical velocity through the cloud and humidity fields. The correlation of broadband OLR and tropospheric temperature is generally small over short time scales and more significant over land than over water. The GCM wind–OLR correlation is a maximum for bandpass waves of synoptic (spherical harmonic wavenumber 8–15) dimension, but it shows only a small variation with the temporal or spatial scale or with the height of the wind. Stratiform clouds are found to have a dominant impact on the model OLR fluctuations, even over much of the tropics.

1. Introduction

The correlation of atmospheric radiation to dynamical and physical variables has long been recognized as a fundamental aspect of meteorology. The classical air mass description of synoptic meteorology contains an inherent correlation of top-of-the-atmosphere radiation to large-scale dynamics: The midlatitude cyclones develop cloud forms, which affect the emitted- and reflected-radiation fields. The earliest satellite observations qualitatively substantiated the air mass theory of the relation of cumuliform and stratiform cloudiness to frontal structure and vortex development. While there has been considerable progress (beginning with Winston 1967) in relating satellite-observed radiances to circulation on longer time scales, the classical short-time scale picture remains subjective for want of extensive datasets which will permit radiation and cloudiness on the global scale to be simultaneously correlated with the large-scale dynamics observed by the radiosonde network. Recent observations (Cahalan et al. 1982) and model results (Charlock et al. 1988) agree in placing the dominant radiative variability in the briefer temporal scales. An extensive International Satellite Cloud Climatology Project (ISCCP) is presently attempting to generate a data set which will be valuable for studying the interactions between clouds, radiation, and dynamics (Schiffer and Rossow 1985).

This paper describes some of the essential relations between the short period, weather-scale fluctuations among radiative, dynamical, and physical variables in a general circulation model (GCM); satellite and National Meteorological Center (NMC) data are also used when appropriate. The techniques used here include cross-correlation and partial-correlation analysis with temporal filters and spherical harmonic analysis applied to key fields. We have emphasized the use of a model, not merely because presently available data are limited, but because these techniques provide considerable insight into the physical processes in the model. We hope to assist model development in an important area by suggesting the tools needed for model validation and diagnosis.

A slightly modified (Charlock and Ramanathan 1985) version of the NCAR Community Climate Model (Pitcher et al. 1983; Ramanathan et al. 1983; and Malone et al. 1984) is used here. This is a spectral GCM (15 wavenumbers). We consider a perpetual January, fixed sea-surface temperature simulation of

Corresponding author address: Dr. Thomas P. Charlock, M.S. 420, Atmospheric Sciences Division, NASA Langley Research Center, Hampton, Virginia 23665-5225.

120 days duration. The model clouds, water vapor, and temperatures influence the transfer of radiation, with a full-radiative transfer routine being done every 12 hours. Clouds are generated when the relative humidity in a layer exceeds 0.80. Stratiform cloud (with an areal coverage of 0.95) or convective cloud (area 0.30) is specified, depending on whether or not the convective adjustment routine is also called in a given time step. In the present version of the GCM, the optical properties of the clouds are computed as functions of the variable cloud liquid water contents. The cloud optical properties in the standard version are constants. A height restriction on cirrus cloud formation in the standard version was relaxed here.

The simulation of the outgoing longwave radiation (OLR) in the present version of the GCM is described in Charlock et al. (1988); it is quite similar to that in the standard form of the model. Many of the principal features of the observed time-mean radiation field are fairly well simulated by the GCM. The temporal standard deviation of the model OLR over fixed points is larger than that found in the satellite record. Over the tropics, the autocorrelation of the model OLR is too low. The spatial gradients of OLR standard deviation and autocorrelation in the GCM are quite realistic, however. The model time series reveal that fluctuations in cloudiness force the bulk of the short-term variations in the OLR over most grid points. The short-term variations in OLR produced by changes in clear-sky opacity (due to variations in water vapor) or temperature are generally smaller than the variations produced by clouds.

This GCM lacks a diurnal cycle. Low-level clouds may be especially influenced by the diurnal cycle, and the low-level clouds can be highly reflective to incoming solar radiation. We will, therefore, restrict the analysis to the OLR, where the lower clouds have a smaller effect. For similar reasons, we will confine most of our discussion to the oceans rather than the continents.

Section 2 will present the cross correlations of the poleward component of the wind and the OLR; this is the classical picture of the influence of midlatitude troughs on cloud patterns. Section 2 will also compare model and observations using time filters. In section 3, the relation between OLR, vertical velocity, precipitable water, and cloudiness will be explored. An overall assessment will be given in section 4.

2. Cross correlation between OLR and the poleward component of the wind

In Fig. 1a, we show the cross correlation between the OLR and the poleward component of the wind at sigma level 0.664 (approximately 664 mb). This level has been selected because of its steering influence on many cloud patterns (Cahalan et al. 1982). The OLR and wind fields have been subjected to a bandpass filter (Blackmon 1976) to isolate the periods of 2.5 to 6 days: the synoptic waves. We notice in Fig. 1a, large areas of the middle latitudes of both hemispheres, especially the storm tracks, where the cross correlation of poleward wind and OLR falls below −0.4. The strongest correlations in the Northern Hemisphere are produced over the centers of the North Atlantic and North Pacific Oceans. A large negative correlation between OLR and the poleward wind is also seen over the Mediterranean Sea. The correlation in Fig. 1a vanishes in the tropics. A continuous belt of high negative correlation is found in the middle latitudes of the Southern Hemisphere.

The negative correlation in Fig. 1a is explained by the classical picture of a midlatitude geopotential wave and the cloudiness associated with it. At the leading edge of a trough, the poleward component of the wind is positive. The leading edge is associated with uplift and a tendency to form clouds. The clouds depress the OLR, yielding a negative correlation between the poleward wind and the OLR. The poleward wind is also positively correlated with air temperature, which alone, would tend to give a positive (opposite to the sign of the cloud effect) correlation between the poleward wind and the OLR. The cloud effect generally predominates over the oceans.

Over land, however, the surface will rapidly heat or cool in response to the air advected by the wind. The surface is a very effective emitter of infrared radiation. The land surface can substantially add to the increased atmospheric infrared emission which is produced by the warm air advected by a positive poleward wind. The correlation of poleward wind and OLR by this land effect would then be positive. Figure 1a shows several areas in continental interiors where the poleward wind and OLR correlation, which by the cloud effect would be negative, has approached zero or become positive.

The model relationships in Fig. 1a are difficult to verify in the real atmosphere because of the lack of suitably long global datasets with radiation and dynamics determined simultaneously. Both the poleward component of the wind and the OLR are observed routinely, but not at the same times. Over the midlatitude storm track, where some of the strongest cross correlations between radiation and dynamics are obtained, the autocorrelation of OLR vanishes within 24 hours for both the observed (Cahalan et al. 1982) and modeled (Charlock et al. 1988) fields. The short autocorrelation of OLR poses serious problems in relating dynamics to radiation with a dataset derived from the available polar orbiter data. There can be a difference of up to 6 hours between the satellite and the 00 and 12 UTC radiosonde observations. We have made an heuristic attempt to circumvent this with the 2.5- to 6.0-day bandpass filter. In Fig. 1b, both the observed OLR and the NMC 700-mb poleward wind fields were filtered before cross correlating. Data from two winters

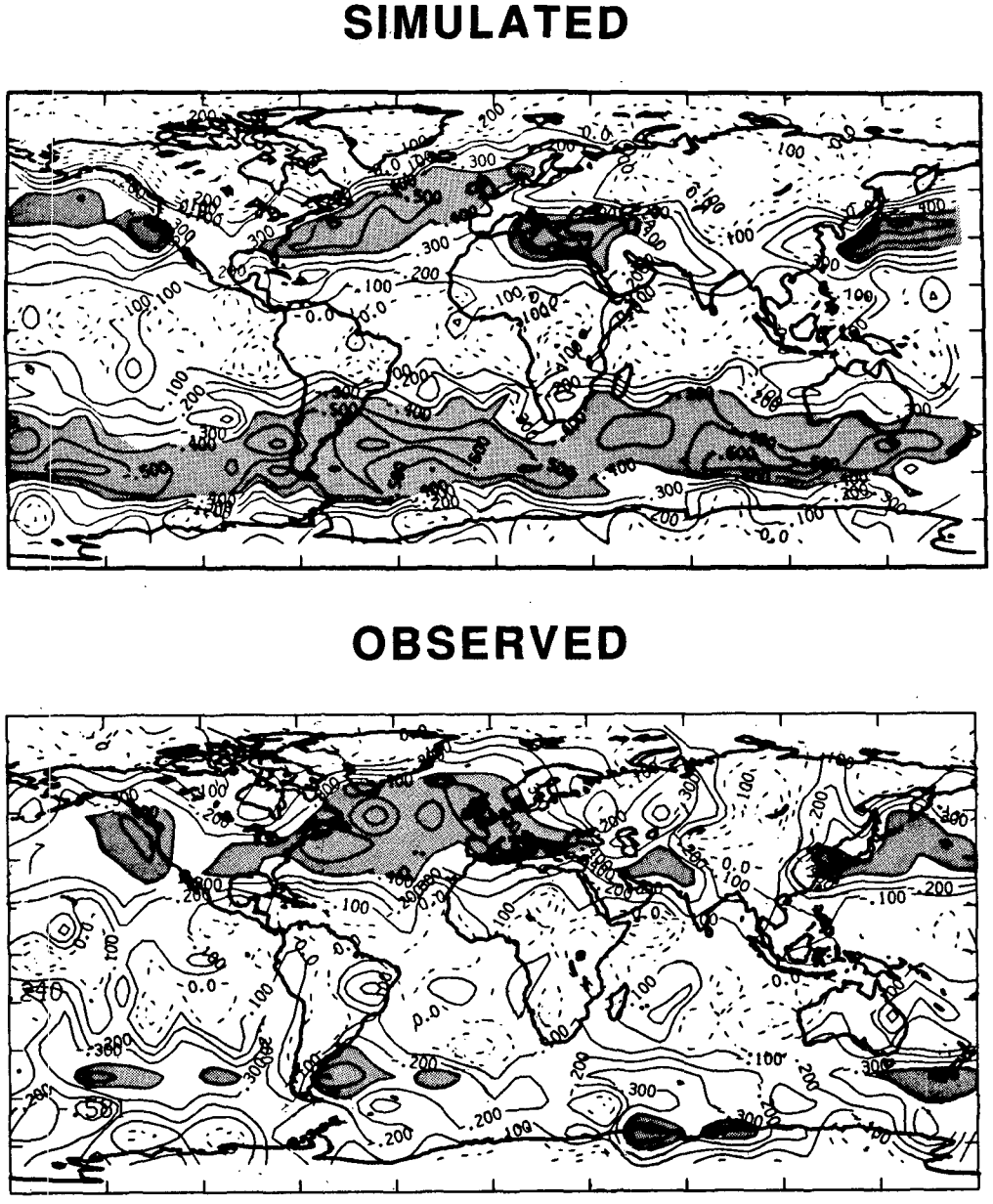

FIG. 1. (a) Cross correlation of the poleward component of the wind at sigma level 0.664 with the OLR in the GCM. Both fields bandpass (2.5–6.0 day) filtered. Positive contours dashed. Shading for correlations less than −0.4. (b) Observed poleward component of NMC 700 mb wind and AVHRR OLR, bandpass (2.5–6.0 day) filtered and cross correlated. Dashes and shading as in (a).

(Jan–Feb 1979 and Dec 1979–Jan–Feb 1980) were used. The seasonal cycle was removed from the data with a quadratic least squares fit.

The OLR was obtained from the NOAA Heat Budget record (Gruber and Krueger 1984), which uses the narrowband AVHRR instrument and a model to produce the broadband OLR. The Nimbus-7 ERB scanner (Jacobowitz et al. 1984) broadband OLR cannot be used for this purpose because of the intermitancy of its data record. The narrowband AVHRR does not capture the full variance of the broadband OLR time series over a given point, probably because it does not cover the water vapor channels adequately. Here, as we have pointed out, we are looking primarily for a cloud effect, which the AVHRR can retrieve. The geographical gradients of the OLR standard deviations in the AVHRR (narrowband) and Nimbus 7 (broadband) match well, as do the autocorrelations, and the

AVHRR is a suitable surrogate here (Charlock et al. 1988).

The magnitudes and geographical variations of the modeled and observed bandpass cross correlations in Fig. 1 are strikingly similar in the Northern Hemisphere. The GCM cross correlations are larger than the observed values in the Southern Hemisphere. It is suspected that some of the differences in the Southern Hemisphere are due to the sparcity of the radiosonde observations rather than to a model deficiency.

Earlier work (Charlock et al. 1988), showed that while the observed autocorrelations of OLR are modeled quite well in the midlatitude storm track, the model standard deviation for the OLR is 50 to 100 percent larger than the observed standard deviation over the globe generally. It appears that while the magnitudes of the OLR fluctuations are too large in the model, the phasing of the OLR with the dynamics (Fig. 1) is correct in the midlatitudes. The top-of-the-atmosphere OLR fluctuations also indicate radiative diabatic fluctuations within the atmosphere; the OLR may further serve as an analog for condensational diabatic heating. The effect of these diabatic fluctuations upon the model dynamics is more uncertain. Pitcher et al. (1983), Ramanathan et al. (1983), and Malone et al. (1984) have demonstrated that the model dynamical simulation is quite sound over many of various temporal and spatial scales. The model may be overly baroclinic, however, in the bandpass time scale (see Malone et al. 1984, Fig. 19b; and Blackmon et al. 1979, Fig. 3b) over much of the area where OLR correlates well with dynamics.

We now examine the correlation of Fig. 1a in a different temporal, and then a different spatial, domain. Figure 2 shows the cross correlation of the poleward wind at sigma level 0.664 and OLR from the GCM with both fields subjected to a high-pass filter (Blackmon 1976) which isolates the effects of the short-period (1- to 2-day) waves. The more east–west elongation of the patterns in high-pass (Fig. 2) in contrast to those of bandpass (2.5- to 6-day, Fig. 1a) is produced by small disturbances which are superimposed on the zonally oriented jets of both hemispheres. The area covered by such small disturbances (Fig. 2) is relatively larger in the Northern Hemisphere, which in January has the stronger jet. The cross-correlation extrema in the Northern Hemisphere correspond with the exit regions of the tropospheric jets. In both hemispheres, the cross correlations using the high-pass filter taper off more quickly than do the correlations using the 2.5- to 6-day bandpass filter as we move from the midlatitudes into the tropics.

The unfiltered cross correlation of the poleward wind at sigma level 0.664 and OLR in the GCM (not shown) has negative values of slightly smaller absolute magnitude, but over larger areas, than in the filtered fields of Figs. 1a and 2. This is apparently a characteristic of the larger, long-period waves. In order to examine the correlation for such planetary waves, the model wind and OLR were projected using spherical harmonics, truncated to degree 7, and then regridded. The cross correlations of these planetary waves are shown in Fig. 3. It is notable that the correlation patterns have diminished only slightly (roughly by 0.1 from the unfiltered and 0.2 from the filtered) in most locations. The most distinguished shift is found in the subsidence zone to the west of South America. The modest correlation between the poleward wind and the OLR is also a robust one, occurring in various temporal and spatial scales over the same geographical regions. The most distinct correlation pattern, smallest minima and largest maxima, is produced from the bandpass (2.5- to 6-day) filtered, medium size (spherical harmonic degree 8 through 15) waves.

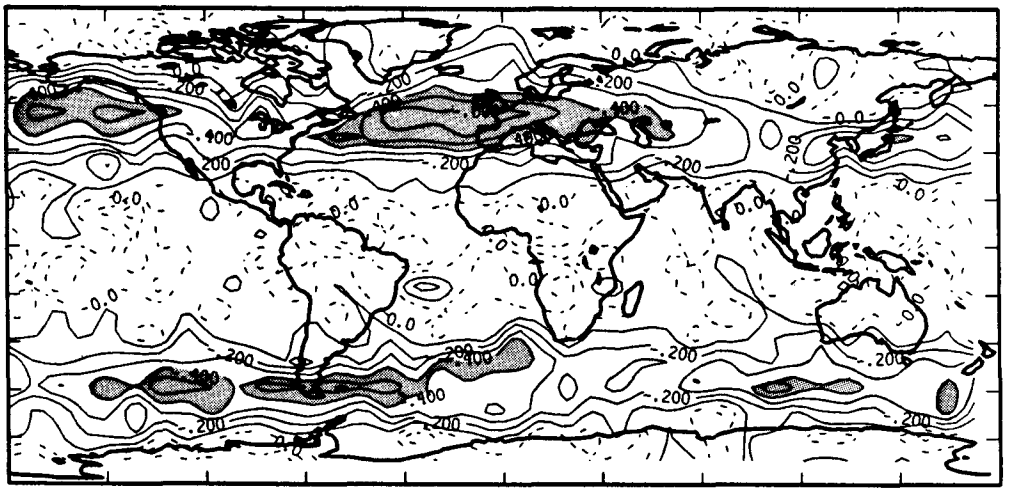

FIG. 2. As in Fig. 1a, but both model fields highpass (1–2 day) filtered. Dashes and shading as in Fig. 1a.

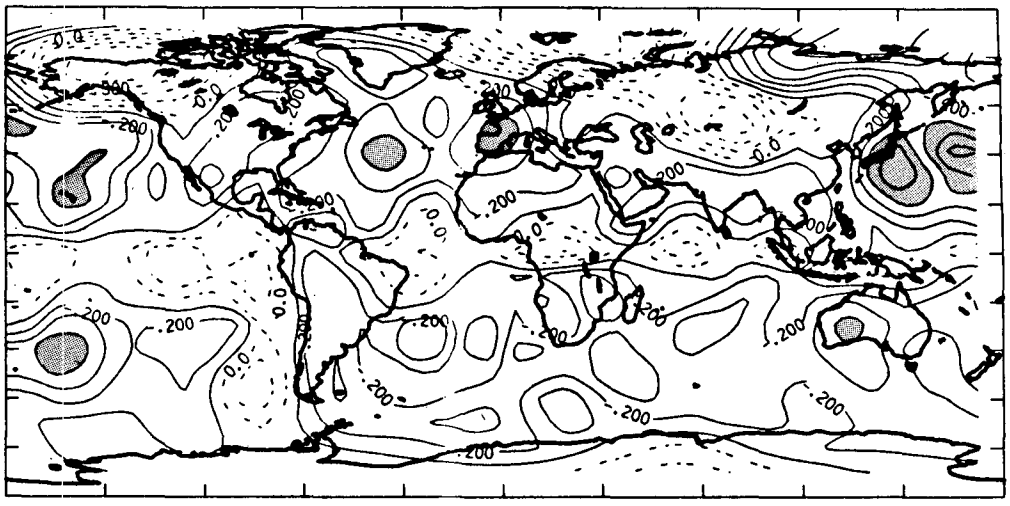

FIG. 3. Cross correlation of the poleward component of the wind at sigma level 0.664 with the OLR in the GCM. Both fields expressed to spherical harmonic degree 7. Dashes and shading as in Fig. 1a.

Relationships similar to those of Fig. 1 were found among other fields. The poleward wind–OLR relation was found to be weaker at other vertical levels. At sigma level 0.336 (approximately 336 mb) the correlations diminished by about 0.1 from those at sigma level 0.664. The cross correlation between the OLR and the zonal wind (not shown) is generally smaller than that with the poleward wind because fluctuations in the zonal wind are not as sensitive an indicator of midlatitude wave activity as are fluctuations in the poleward component.

At each model grid point, a clear-sky radiation calculation was performed. The clear-sky OLR was recorded, regardless of the occurrence or nonoccurrence of clouds in a given time step. Over the oceans, we find that changes in cloudiness force most of the short-time scale variance in the regular, full-sky (clear plus clouds if any) OLR; changes in humidity and temperature force the variance in the clear-sky component. This clear-sky OLR field was cross correlated with the poleward component of the wind at sigma level 0.664. The resulting pattern (not shown) was only slightly different from Fig. 1a or 2, depending upon the temporal filter which was applied. This is the case because in the midlatitudes, where coherent relationships between OLR and the poleward wind are found, similar forcings affect both the clear-sky and full-sky OLR fields. These forcings may be diagnosed by considering the complex interplay of the OLR with the cloud, humidity, and vertical velocity fields.

3. Cloudiness, water vapor, and vertical velocity

Clouds play the dominant role in forcing changes in OLR for short time scales over most of the globe. This is demonstrated in Fig. 4, which maps the cross correlation between the full-sky OLR and a stratiform cloud index. The stratiform cloud index was formed by simply flagging the GCM history tapes in each time step with 0.0 for no stratiform clouds and 1.0 for stratiform clouds in any level except the lowest, where clouds do not influence the model radiation. One-half of the variance in the OLR over large regions of the midlatitudes is explained by this crude index, which is independent of the height of the clouds. Little change is found in the correlation patterns of Fig. 4 when the fields are high-pass filtered (not shown), indicating the pronounced impact of stratiform clouds on the model OLR on the shortest time scales, even in the tropics.

Due to the frequency of model moist convective adjustment in the tropics, convective cloudiness had been the suspect for producing the lower than observed autocorrelation in tropical OLR which was mentioned earlier. Convective parameterizations using the Kuo (Donner 1986) and other (Albrecht et al. 1986) techniques have been actively investigated with this model. The convective analog to Fig. 4 shows only a few contours of magnitude −0.3, and these are found mostly in the midlatitudes. The model stratiform clouds have a much greater impact on the OLR over most of the globe than do the convective clouds. This is because the areal coverage of convective clouds (0.30 when they form) is smaller than that of stratiform (0.95) in the model. It is possible, however, that the temperature and moisture regime, which is partly forced by the present convective adjustment scheme, indirectly induces overly active stratiform clouds in the model tropics. A comparison (Charlock et al. 1988) of the modeled and observed time-mean OLR fields indicates that the model needs more high cloudiness over Indonesia, the Amazon, and southern Africa. Perhaps the model could be rectified with a deep-convection

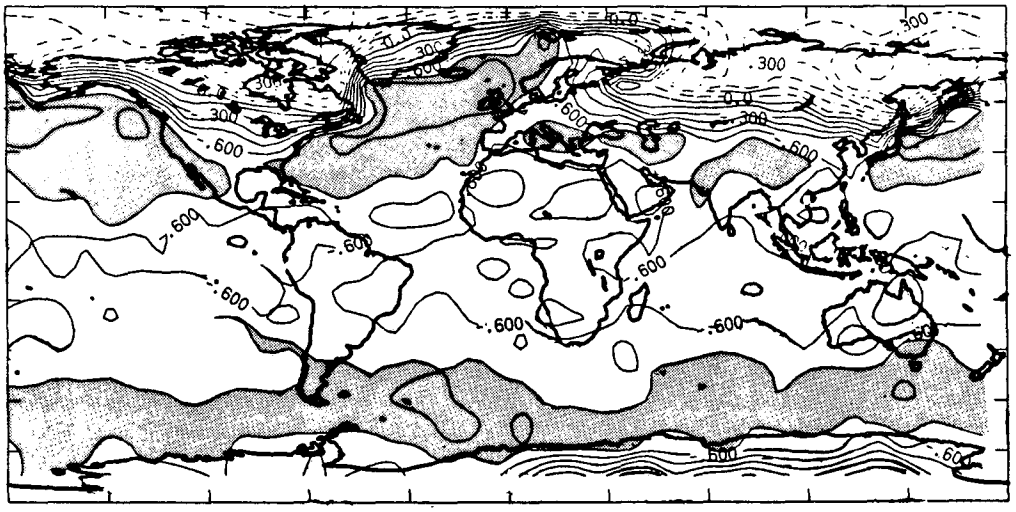

FIG. 4. Cross correlation of model OLR with stratiform cloud index. Dashes for positive contours. Shading for values below −0.7.

parameterization that also forms persistent high stratiform clouds of large area; the new parameterization would be activated under more stringent conditions than those for the present convective adjustment. The areal coverage of other stratiform clouds in the tropics should be reduced in the model. (Other speculations on means for improving the cloud parameterizations are found in Charlock et al. 1988.)

The close match of the modeled and observed cross correlations of radiation and dynamics (Figs. 1a and 1b) gives some confidence, at least in the midlatitudes, in the generating mechanisms for the GCM clouds, which force most of the variance in the OLR (Fig. 4). The clouds are formed mostly in response to the fluctuations in humidity and vertical velocity in the model.

The specific humidity field in the GCM was split into low (sigma levels 0.991, 0.926, and 0.811), middle (0.664, 0.500, and 0.336), and high (0.189, 0.024, and 0.009) levels for analysis. The middle tropospheric water vapor has the greatest impact on the OLR, and this cross correlation is shown in Fig. 5a. Simply stated, more moisture tends to mean more clouds. The clouds decrease OLR, accounting for the predominantly negative contours in the map. For the middle-level water vapor, we obtain values of −0.5 over most of the global ocean. Recall that the poleward wind exhibited cross correlations of −0.4 with the OLR in especially active areas only. Clear-sky influences are similar over much of the globe (Fig. 5b). A positive excursion in the middle level moisture field is associated with a larger clear-sky opacity variation than is obtained with a proportionate increase at a higher level, where there is less water. The lower troposphere has more moisture, but there the temperature contrast with the strongly emitting surface is smaller. Figure 5b (clear sky) cross correlations generally exceed those of Fig. 5a (full sky); in the full-sky case, middle level humidity variations are often uncorrelated with cloud fluctuations at other levels, which can substantially affect the OLR.

Geographical effects are pronounced in Fig. 5. Over the Northern Hemisphere continents (January simulation), the correlation switches to positive in the high latitudes, with fluctuations in surface emission dictating the sign of the correlation; episodes of high (low) temperature are correlated to high (low) surface emission, and also to high (low) water vapor mixing ratio. Variations in the opacity of the atmosphere, as opposed to actual emission from the surface, play less of a role in high latitude OLR because 1) the atmospheric opacity is itself reduced near the poles, and 2) the vertical temperature lapse rate is low. The shift from positive to negative cross correlation occurs at lower latitudes in the clear-sky map (Fig. 5b), wherein clouds do not mask changes in land-surface emission.

An increase in the temperature at a particular level in the atmosphere, with all other factors constant, would increase the OLR. The cross correlation of middle tropospheric temperature and OLR is small. This correlation is slightly negative over the midlatitude oceans because warmer air generally contains more water vapor, which blocks the infrared emission from the sea surface.

What produces the excursions in middle level tropospheric humidity which correlate so well with the OLR? In the midlatitudes, the answer appears to be found in the large scale vertical velocity field. We consider the vertical velocity as a time derivative of pressure, so it is positive downwards. The vertical velocity at sigma level 0.664 may coarsely be considered as a pump for the middle tropospheric precipitable water

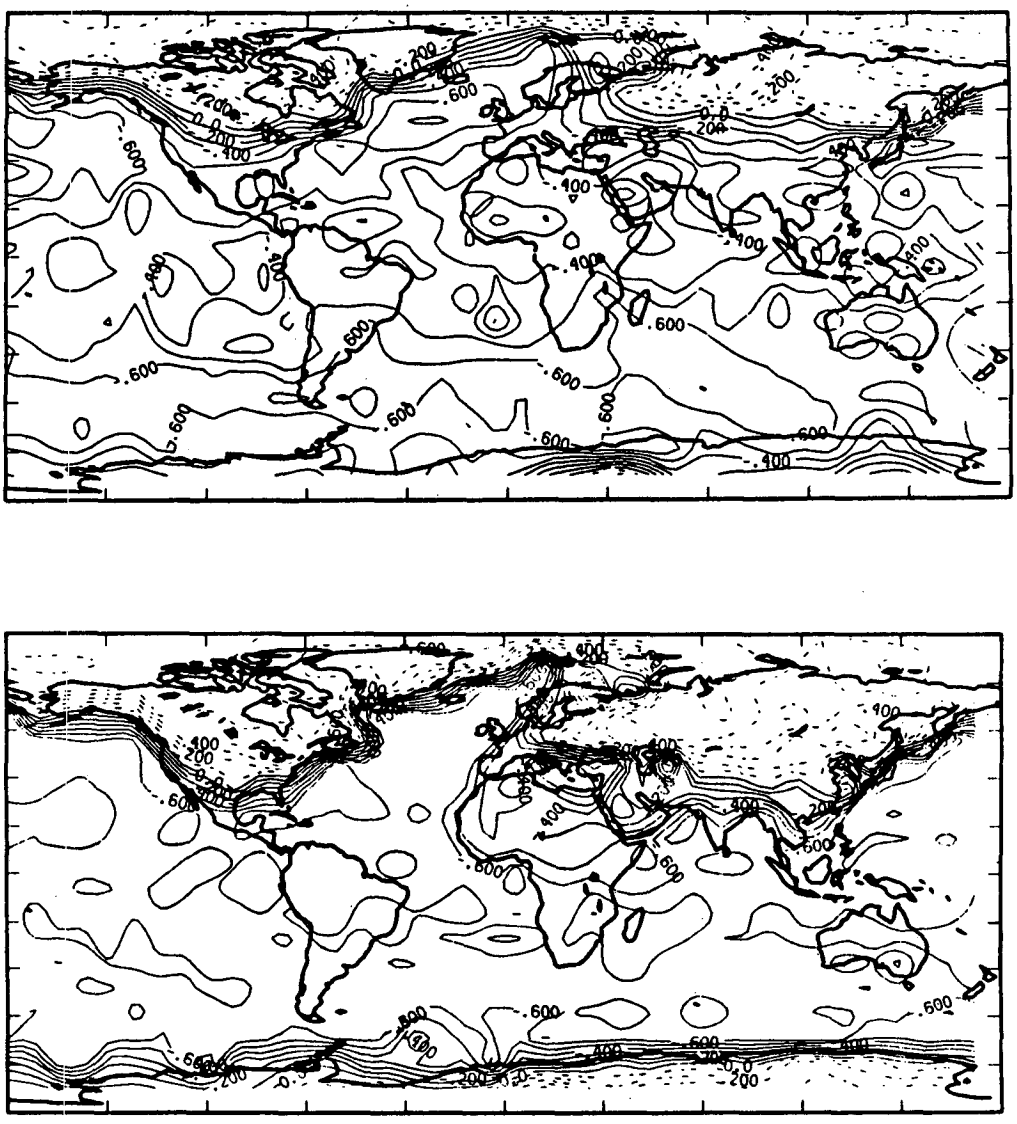

FIG. 5. (a) Cross correlation of model OLR and middle level tropospheric precipitable water. Dashes for positive contours. (b) As in (a) but for model clear-sky OLR. Dashes as in Fig. 5a.

at sigma levels 0.664, 0.500, and 0.334. Figure 6 displays the cross correlation of the vertical velocity at sigma level 0.664 with the OLR. In the midlatitude storm tracks, the +0.6 contour of Fig. 6 (vertical velocity–OLR) and the −0.6 contour in Fig. 5a (middle level humidity–OLR) match closely; in the tropics the humidity explains more of the variance in the OLR than does the vertical velocity. The cross correlation of vertical velocity and precipitable water (not shown) indicates a significant relationship in the midlatitudes.

In Fig. 7, we show the partial correlation of OLR and middle level precipitable water with the vertical velocity at sigma level 0.664 held constant. Figure 7 is the partial correlation analog of Fig. 5a. By holding the vertical velocity constant, we diminish the cross correlation of OLR and middle level precipitable water considerably. The partial correlations could then be associated with the transport of water vapor either by 1) horizontal winds or 2) vertical velocity at sigma levels other than 0.664. The partial correlation of OLR and the poleward component of the wind (sigma level 0.664) with vertical velocity held constant was computed and found to be significantly below 0.0 hardly anywhere. This suggests that the second mechanism is the more dominant.

4. Conclusions

It is shown that the observed and modeled bandpass cross correlation of the poleward wind and the OLR

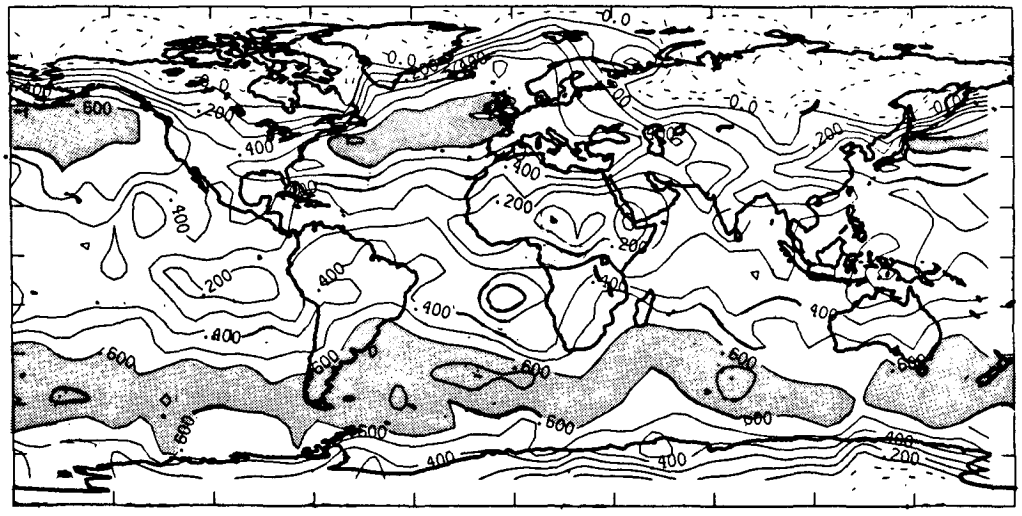

FIG. 6. Vertical velocity at sigma level 0.664 in the model cross correlated with OLR in the model. Dashes for negative contours. Shading for values over 0.6.

in the midlatitude storm track match quite closely. This demonstrates that we can use large-scale models to simulate and understand the fluctuations of radiation and dynamics in certain respects.

The model dynamics exert a coherent impact on the full-sky OLR in the midlatitudes largely by generating the stratiform clouds. The dynamics also control much of the short-term variance in the model clear-sky OLR by the vertical pumping of water vapor. An analysis of partial correlations showed that almost all of the tendency of the poleward component of the wind to influence OLR is through its impact on the vertical velocity field; the horizontal advection of moisture by that wind is evidently not as important over short-time scales. The vertical velocity may directly force the formation of an opaque cloud, or it may merely pump up the precipitable water and increase the convergence of water vapor into the column; either effect induces the same sign of the correlation between vertical velocity and OLR.

The substantial role played by stratiform clouds in forcing variations of OLR in the model tropics, even on the shorter time scales, was also interesting. The impact of convection on the model OLR is certainly not large in the direct sense over many areas.

Acknowledgments. We thank B. Briegleb for assistance in procuring the GCM data used in this work.

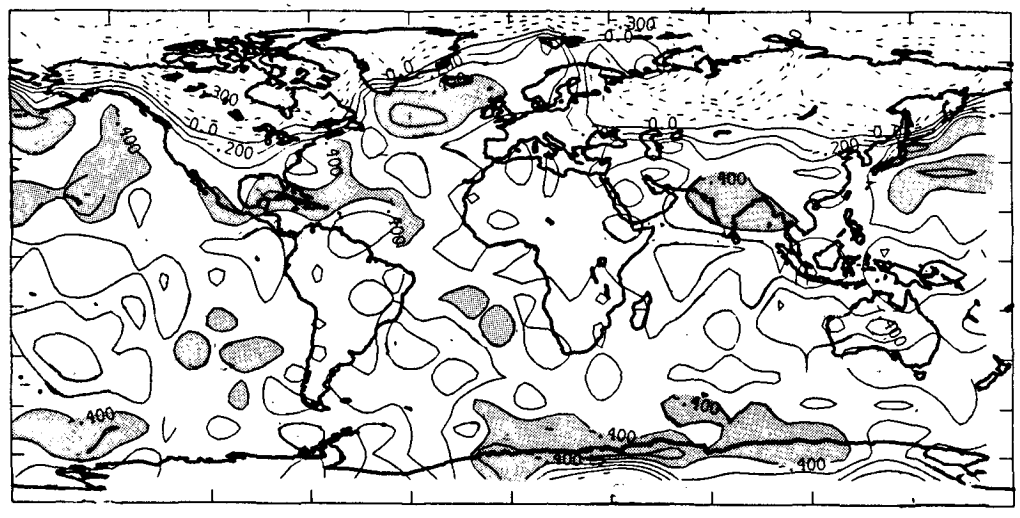

FIG. 7. Model partial correlation of OLR and middle level precipitable water with vertical velocity at sigma level 0.664 held constant. Dashes for positive contours. Shading for values below −0.4.

We are especially grateful to G. L. Smith, whose careful review of an earlier draft led to an improvement of this paper. Useful discussions were provided by L. Donner, J. T. Suttles, and T. D. Bess. The critical comments of two anonymous reviewers are appreciated.

REFERENCES

Albrecht, B. A., V. Ramanathan and B. A. Boville, 1986: The effects of cumulus moisture transports on the simulation of climate with a general circulation model. *J. Atmos. Sci.*, **43**, 2443–2462.

Blackmon, M. L., 1976: A climatological spectral study of the 500 mb geopotential height of the Northern Hemisphere. *J. Atmos. Sci.*, **33**, 1607–1623.

——, R. A. Madden, J. M. Wallace and D. S. Gutzler, 1979: Geographical variations in the vertical structure of geopotential height variations. *J. Atmos. Sci.*, **36**, 2450–2466.

Cahalan, R. F., D. A. Short and G. North, 1982: Cloud fluctuation statistics. *Mon. Wea. Rev.*, **110**, 26–43.

Charlock, T. P., and V. Ramanathan, 1985: The albedo field and cloud radiative forcing in a general circulation model with internally generated cloud optics. *J. Atmos. Sci.*, **42**, 1408–1429.

——, K. M. Cattany-Carnes and F. Rose, 1988: Fluctuation statistics of outgoing longwave radiation in a general circulation model and in satellite data. *Mon. Wea. Rev.*, **116**(9), 1540–1554.

Donner, L. J., 1986: Sensitivity of the thermal balance in a general circulation model to a parameterization for cumulus convection with radiatively interactive clouds. *J. Atmos. Sci.*, **43**, 2277–2288.

Gruber, A., and A. F. Krueger, 1984: The status of the NOAA outgoing longwave radiation data set. *Bull. Amer. Meteor. Soc.*, **65**, 958–962.

Jacobowitz, H., R. J. Tighe and The NIMBUS 7 ERB Experiment Team, 1984: The Earth radiation budget derived from the NIMBUS 7 ERB experiment. *J. Geophys. Res.*, **89**, 4997–5010.

Malone, R. C., E. J. Pitcher, M. L. Blackmon, K. Puri and W. Bourke, 1984: The simulation of stationary and transcient geopotential-height eddies in January and July with a spectral general cirulation model. *J. Atmos. Sci.*, **41**, 1394–1419.

Pitcher, E. J., R. C. Malone, V. Ramanathan, M. L. Blackmon, K. Puri and W. Bourke, 1983: January and July simulations with a spectral general circulation model. *J. Atmos. Sci.*, **40**, 580–604.

Ramanathan, V., E. R. Pitcher, R. C. Malone and M. L. Blackmon, 1983: The response of a general circulation model to refinements in radiative processes. *J. Atmos. Sci.*, **40**, 605–630.

Schiffer, R. A., and W. B. Rossow, 1985: ISCCP global radiance data set: A new resource for climate research. *Bull. Amer. Meteor. Soc.*, **66**, 1498–1505.

Winston, J. S., 1967: Zonal and meridional analysis of 5-day averaged outgoing long-wave radiation data from TIROS IV over the Pacific sector in relation to the Northern Hemisphere circulation. *J. Appl. Meteor.*, **6**, 453–463.